

Performance Of A Compact Gamma Tube Interrogation Source

Michael J King^{1,2}, Arlyn J Antolak¹, Ka-Ngo Leung^{2,3}, Dan H Morse¹, Thomas N Raber¹, Barney L Doyle⁴

⁽¹⁾*Sandia National Laboratories, Livermore CA*

⁽²⁾*Nuclear Engineering Department, University of California, Berkeley CA*

⁽³⁾*Lawrence Berkeley National Laboratory, Berkeley CA*

⁽⁴⁾*Sandia National Laboratories, Albuquerque, NM*

Abstract. Active interrogation with high-energy monoenergetic gammas can induce photofission signals in fissile materials while minimizing absorbed radiation dose and background from surrounding materials. A first-generation axial-type gamma generator has been developed that utilizes the $^{11}\text{B}(p,\gamma)^{12}\text{C}$ nuclear reaction at a 163 keV resonance to produce monoenergetic 12-MeV gamma-rays. The gamma tube employs a water-cooled cylindrical radio frequency (rf) induction ion source capable of producing a proton current density of up to 100 mA/cm². The extracted proton beam bombards a lanthanum hexaboride (LaB₆) target at energies up to 200 keV. The 12-MeV gamma intensity was measured as a function of proton energy, beam current, and angle. Photofission-induced neutrons from depleted uranium (DU) were measured and compared to MCNPX calculations. After extended operation, the high power density of the proton beam was observed to cause damage to the LaB₆ target and the gamma tube improvements currently being made to mitigate this damage are discussed.

Keywords: photofission, active interrogation, gamma generator

PACS: 52.38.Ph, 87.50.Gi, 29.17.+w, 25.20.-x

1. INTRODUCTION

Detecting and verifying concealed or shielded fissionable material is a challenging problem. Conventional passive methods rely on spectroscopy of the low-energy gamma-rays from natural decay, but this approach is not viable when thick shielding is present. Alternatively, photonuclear active interrogation techniques¹ can penetrate shielding and generate detectable higher energy fission signatures. These techniques utilize high energy photons from an electron linear accelerator where most of the photons are too low to induce photonuclear reactions and only contribute to a higher background dose.

Recently, a new axial-type mono-energetic gamma tube generator was developed that uses low-energy nuclear reaction resonances to produce high-energy gammas.² In particular, the gamma tube uses the

$^{11}\text{B}(p,\gamma)^{12}\text{C}$ nuclear reaction which has a resonance in its cross section at 163 keV and produces 12-MeV gamma-rays which are near the peak of the photofission cross section. This paper describes experiments performed to assess the operational performance of the gamma tube. The intensity of the 12-MeV gamma-rays from the generator was measured as a function of proton energy, beam current, and angle. Photofission-induced neutron rates in depleted uranium (DU) were measured and compared to MCNPX calculations. It was later discovered that the high power density of the proton beam caused significant beam damage to the LaB₆ target. Improvements to the gamma tube are discussed that will reduce the power density and damage to the target.

2. AXIAL TYPE GAMMA TUBE

The gamma generator (see schematic and photo in Fig. 1) utilizes an rf induction ion source, a multi-electrode acceleration column, and boron-containing target.² The $^{11}\text{B}(p,\gamma)^{12}\text{C}$ nuclear reaction has a well-known resonance at 163 keV proton energy, having a

cross section of $156\ \mu\text{b}$ and width of 7 keV. The reaction produces a pair of 4.4-MeV and 11.7-MeV gammas 97% of the time and 16.1-MeV gammas 3% of the time. Both the 11.7-MeV and 16.1-MeV gammas are above the threshold for photofission which is approximately 6-MeV. These high energy photons will induce the photofission neutrons necessary for hidden nuclear material detection.

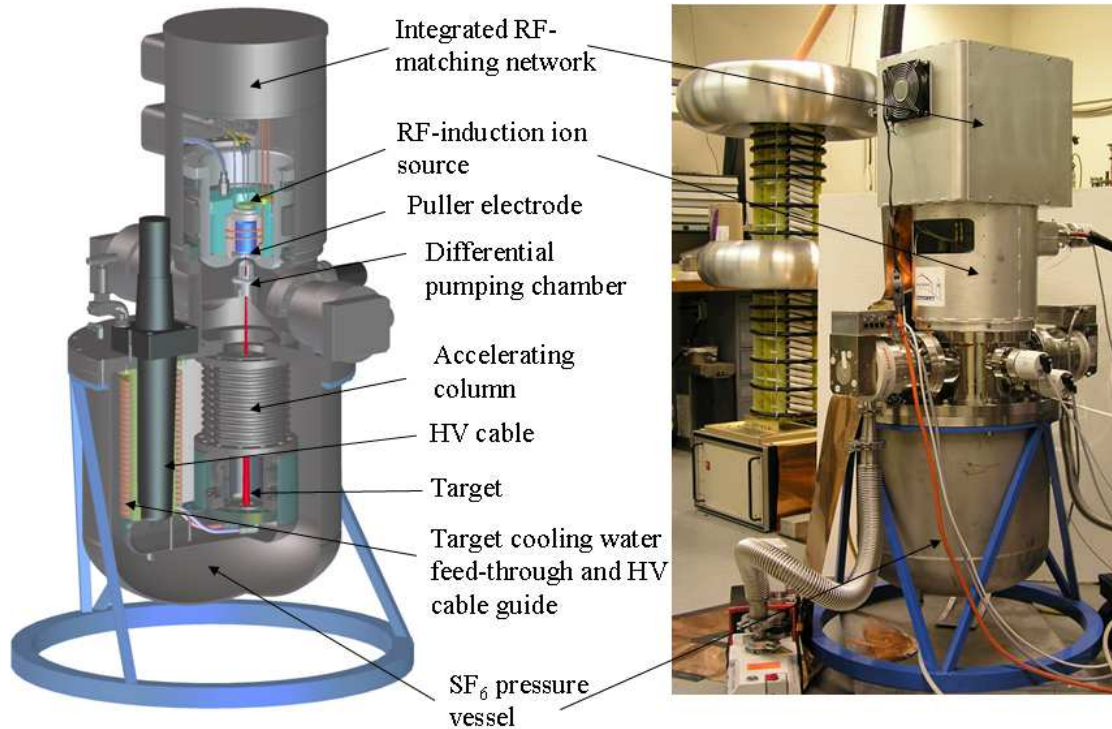


FIGURE 1. On the left is a cut-away schematic of the axial-type gamma tube. On the right, the gamma tube is shown in the laboratory with the high voltage power supply behind it. The dimensions of the gamma tube are 40 cm in diameter and 100 cm in height.

The 163 kV voltage needed for the reaction necessitated the use in the gamma tube of an acceleration column, differential pumping system, and pressurized vessel that could enclose the high voltage column. Several boron-containing materials were initially considered for the gamma tube target including sintered boron carbide (B_4C), natural boron, and lanthanum hexaboride (LaB_6). LaB_6 was selected due to its high thermal conductivity and low resistivity. The target consisted of a 3 mm thick, 5 cm diameter sintered LaB_6 ceramic disk mounted on a copper water-cooled plate with a thin layer of liquid indium-gallium acting as a thermal interface for better heat conductivity.

3. AXIAL GAMMA TUBE PERFORMANCE

Gamma Spectrum

Figure 2 shows gamma spectrum measured from the gamma tube using a 3" x 3" NaI detector. For gammas at these high energies, pair production begins to dominate and the difficulty in fully absorbing the pair products and annihilation photons can be seen in the spectrum.

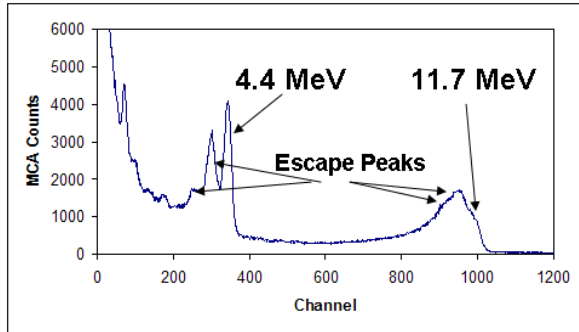


Figure 2. Measured gamma spectrum from the axial gamma tube using a 3'' x 3'' NaI detector. The 4.4 MeV $p\text{-}^{11}\text{B}$ peak produces two lower-energy escape peaks due to pair production. The 11.7 MeV full energy peak is the slight bump near channel 1000 and the 16.1 MeV peak cannot be resolved with this detector. The spectrum was collected for 30 minutes at a beam current of 0.74 mA and acceleration voltage of 169 kV.

Energy detection losses from the production pair's bremsstrahlung emission and lower detection efficiency at higher photon energies contribute to the broadening of higher energy peaks.

Gamma Yield

The process to extract the gamma yield from the measured spectra involved integration and normalization utilizing MCNPX computations. The MCNPX model was initially validated to the measured gamma ray spectrum.³ Figure 3 shows the geometric model for the gamma tube used in the simulations. Most of the materials which have high gamma attenuation coefficients (e.g., metals) in the gamma tube were included in the model while less attenuating materials/structures (e.g., ceramic insulators) were ignored.

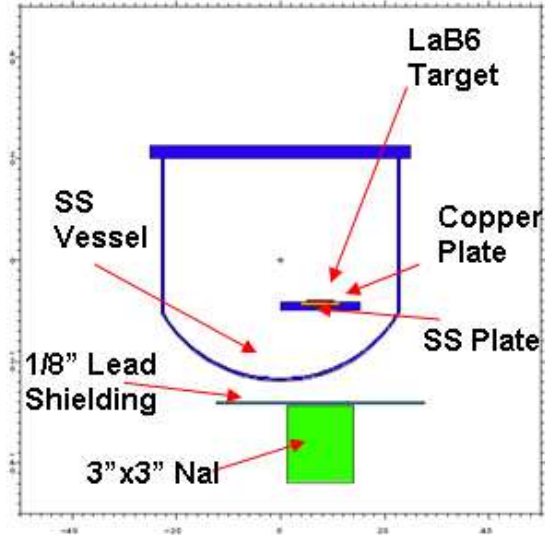


Figure 3. The gamma tube model used in the MCNPX simulations. The model consists of the stainless steel vessel, boron target, copper heat sink, and stainless steel flange. A 3''x3'' NaI detector was modeled with a thin lead sheet on top which helped to attenuate low energy x-rays created from the gamma generator during operation.

For the MCNPX source definition, a Gaussian energy broadening coefficient was defined due to normal energy resolution losses from the NaI detector. These losses can come from non-uniform light collection and photomultiplier noise. The coefficient was estimated by a best-fit method to the experimentally measured spectrum. The deposited energy from all gamma-ray interactions in the detector were tallied and binned. Figure 4 shows the MCNPX computed spectrum compared to experimental result.

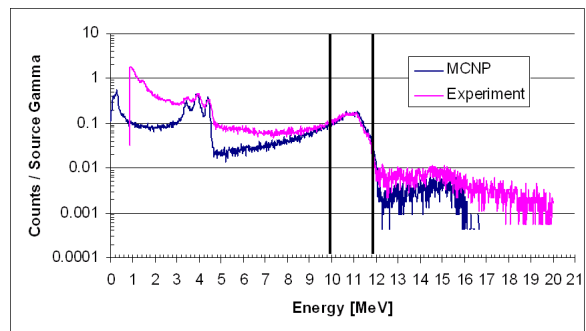


Figure 4. The graph shows the experimental and MCNPX spectra. An energy window, depicted as lines at 10- and 12-MeV, was used to determine the gamma yield.

The simulated spectrum deviates from the experimental result in the range 0 - 3.5 MeV and also in the range 4.4 - 9.5 MeV. The elevated low-energy gamma counts are due to scattering of gamma rays from all materials from the room and gamma tube. The MCNPX simulation does not model all the materials

so a discrepancy occurs at low energies. In the intermediate energies between 4.4 and 9.5 MeV, the discrepancy may originate from thermal neutron capture by ^{35}Cl . The high-voltage cable connector cast material, polyurethane resin, contains chlorine. Because ^{35}Cl has a very high thermal neutron absorption cross section and photoneutrons are created by the gamma rays in surrounding metals, it is very likely the discrepancy is from the gamma decay energies of 6.11, 6.62, 7.41 and 7.79 MeV. The discrepancy between simulation counts and experimental counts scale linearly with the count rate thus eliminating the possibility of chance coincidences. To determine the yield of 11.7 MeV gammas from the LaB_6 target, which will be linearly proportional to the induced photofission neutrons, the experimental spectrum was integrated between 10 and 12 MeV and compared to the integrated MCNPX value. Because the MCNPX output is in units of per source particle (gamma), the computed results could be normalized to the experimental value and time.

The gamma yield as a function of proton current was measured with a 3" x 3" NaI(Tl) detector and yield versus angle measurements were made at different detector orientations using a combination of 3" x 3" and 2" x 2" NaI(Tl) detectors. In the former case, the detector was placed on-axis and 3" below the bottom of the gamma generator pressure vessel corresponding to having the detector 9.25" from the top surface of the LaB_6 target. With 1 mA of beam current, the gamma yield into 4π was measured as 2.0×10^5 γ/s . As seen in Fig. 5, the yield has a slight upward curve at higher beam currents. This non-linear boost in yield can be explained due to an increase in monatomic hydrogen produced by the ion source at higher rf powers.

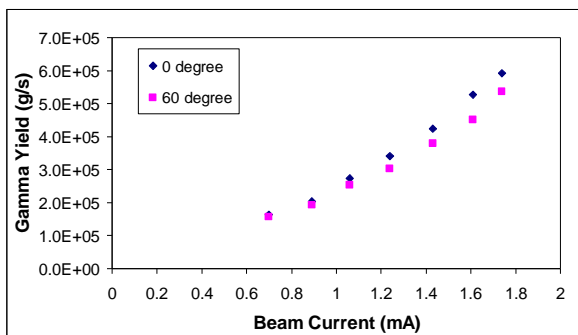


Figure 5. Plot of the measured gamma intensity versus proton current with the detector orientated at two positions relative to the axis of the gamma tube. The bias voltage was 175 kV. Statistical counting errors are smaller than the data point values.

Assuming a best fit line for the yield versus current, the gamma intensity would scale to $\sim 6 \times 10^8$ γ/s for 1 A (average) current using a LaB_6 target. The latter value agrees well with a previous accelerator-based measurement of 1.8×10^7 $\gamma/\text{C-sr}$ using a B_4C target.⁴

Gamma Yield Angular Dependence

The angular dependence of the gammas generated in the gamma tube was measured using a 3"x3" in NaI detector placed at 0 and 60 degrees relative to the proton beam axis, while a 2"x2" NaI detector was kept in a stationary position at 90 degree orientation. The integrated output from the 2" x 2" detector was used to normalize the data collected with the 3" x 3" detector due to the repositioning at different angles. Only the 11.7 MeV gamma-ray was analyzed for the results shown in Fig 3. The average intensity ratio between 60 and 0 degrees was $I_{60}/I_0 = 91\%$ ($\pm 0.7\%$) which is slightly higher than previously calculated and experimental results.^{5,6} An expression for the normalized yield as a function of angle was given as $Y(\theta) \sim 1 + 0.23 \cos^2\theta$ so the expected gamma intensity ratio was 86%.⁶ In order to further corroborate the result, the gamma yield as a function of angle was also measured using an ion accelerator. The target consisted of a disk of 3 mm thick LaB_6 affixed to a 1.5 mm thick aluminum plate. A 3"x3" NaI detector was placed 9" behind the aluminum plate inline with the incident proton beam and a 2"x2" NaI detector was positioned 2" behind the plate at 135° relative to the front surface of the target. Hydrogen ions were accelerated to 400 keV and the total beam current on target was 1.3 μA . In this case, the measured angular intensity ratio was measured to be $I_{60}/I_0 = 86\%$ ($\pm 0.3\%$), which agreed with the gamma tube result.

Photofission Measurements

Depleted uranium was placed directly beneath the gamma tube vessel and approximately 20 cm from the LaB_6 target (see Fig. 6). A 3/16" thick lead sheet separated the uranium from the ^3He detector. The main purpose of the lead was to minimize electromagnetic fields that were created from occasional high voltage sparking from coupling into the detector electronics.

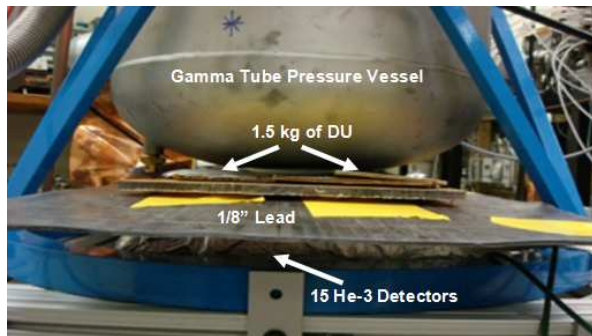


Figure 6. The depleted uranium is immediately below the vessel and on placed on top of a sheet of lead and ^3He neutron detector.

A total of fourteen 116 g disks of depleted uranium were evenly spread out on top of the lead sheet. The neutron detector was comprised of fifteen 1" diameter ^3He tubes placed in a polyethylene moderator with built in preamplifiers.⁷ The intrinsic detector efficiency was estimated with MCNPX to be 2% for 2-MeV fission neutrons. The detected photofission neutron signal was determined subtracting cosmic-induced photoneutrons from DU and lead, decay neutrons from DU, natural room background and photon induced neutrons from the generator while in operation. The natural background count rate was measured to be 2 c/s, and the background count rate with DU and lead in place was 4 c/s. Table 1 shows the measured neutron count rate compared to MCNPX simulation results.

TABLE 1. Neutron count rate as a function of the beam current.

Beam Current (mA)	Measured Neutron Count Rate (n/s)	MCNP Neutron Count Rate (n/s)
0.72	2.6	2.8
1.07	3.7	5.9
1.42	7.8	9.0
1.72	11.3	11.7

In the experiments, the photofission-induced neutron signal could not be distinguished from photon induced neutrons from DU and lead. However, the modeling results show that the photon induced neutrons in lead more than doubled the neutrons produced from the depleted uranium disks.

Boron-Containing Target

The gamma tube maintained stable operation over a period of ~100 hours until some degradation in the gamma output was observed. After disassembling the gamma tube, noticeable beam damage to the LaB_6 target could be seen that was likely caused by the high power density on the target. The beam produced a

crater 3-mm deep and 2-mm in diameter. Power densities of up to 6 kW/cm^2 and temperatures of 2000 K were calculated for the observed 2-mm beam spot on target. X-ray diffraction and Auger analysis determined that the lanthanum to boron ratio did not change inside the crater, no boron migration, although there was a measurable amount of oxygen on the surface.

4. CONCLUSION

The performance of a prototype axial gamma generator has been evaluated through a series of experiments that measured the gamma intensity as a function of proton energy, beam current, and angle. A gamma yield of 2.0×10^5 was measured from the gamma tube using a LaB_6 target with 1 mA of beam current at an energy of 175 kV. By changing to a pure ^{11}B target, the gamma tube is expected to generate 10^6 γ /s with 1 mA of proton current. The angular distribution intensity ratio between 60° and 0° was determined to be 91% ($\pm 0.7\%$) indicating that there is some forward directionality to the generated gammas. Gamma-ray induced neutrons from depleted uranium and lead were detected and validated by MCNPX simulations. A beam extraction electrode modification will be made to the gamma tube that will decrease the power density on the target, increasing the target lifetime, by continuously sweeping the beam across the target surface. Optimizing the ^3He detector module for higher fission neutron detection efficiency and different interrogation setups are planned.

ACKNOWLEDGMENTS

Sandia National Laboratories is a multiprogram laboratory operated by Sandia Corporation, a Lockheed Martin Company, under contract DE-AC04-94AL8500 and at Lawrence Berkeley National Laboratory under contract number DE-AC02-05CH11231. Additional thanks to Miles Clift and Greg Wagner of Sandia National Laboratories for their material analysis work.

REFERENCES

1. J. L. Jones, K. J. Haskell, J. M. Hoggan et al., APPLICATION OF ACCELERATORS IN RESEARCH AND INDUSTRY: 17TH International Conference on the Application of Accelerators in Research and Industry **680**, 947 (2003)
2. J. Reijonen, N. Andresen, F. Gicquel et al., Optics and Photonics in Global Homeland Security III **6540**, 65401P (2007).

3. D.B Pelowitz, *MCNPX User's Manual, Version 2.5.0*, LA-CP-05-0369 ed. (LANL, 2005).
4. Daniel H. Morse, Arlyn J. Antolak, and Barney L. Doyle, Nuclear Instruments and Methods in Physics Research Section B: Beam Interactions with Materials and Atoms **261** (1-2), 378 (2007).
5. Thomas P. Hubbard, Edward B. Nelson, and James A. Jacobs, Physical Review **87** (2), 378 (1952).
6. P. J. Grant, F. C. Flack, J. G. Rutherglen et al., Proceedings of the Physical Society. Section A (9), 751 (1954).
7. Kristin Hertz, Nick Mascarenhas, Matthew Allen et al., Sandia National Laboratory (Sand2005-4261p), 21 (2005).